Astrometric Measurements and Physical Likelihood Assessments for HJ 4258, STF 1106, and VNI 1

Maiya Qiu[1], Nicholas Peh[1], Eden (Songxiao) Li[1], Kalée Tock[1]
[1] Stanford Online High School, Redwood City, CA 94063; maiyaq6487@gmail.com

Abstract

In this study, we analyze historical data and present new astrometric measurements of the position angle and separation of double star systems HJ 4258, STF 1106, and VNI 1 using 10 images for each system. A comparison of HJ 4258's components' relative motions to the computed system escape velocity supports classifying it as a gravitationally bound binary, but the trend in the relative position of its secondary star does not support this, and further research would be needed for confirmation. Similar analysis of STF 1106 and VNI 1 suggests a physical, but not binary, relationship between the component stars of these two systems.

1. Introduction

Double star systems with similar parallax may be gravitationally bound or have some other type of physical relationship. For example, stars in such a pair may have originated from the same nebula, or may share a trajectory in the past or future. Wide double stars systems may also provide information about the structure and evolution of the galaxy and potential gravitational effects of dark matter (Banik et al., 2024). Furthermore, binary systems allow for determination of the mass of each of the stars, which is valuable in refining the mass-luminosity relation, a fundamental tool of astrophysics. In this study, we examine the relationship between the primary and secondary stars for three double star systems whose stars exhibit similar parallax and proper motion.

The systems of this study were chosen from Stelle Doppie, a search engine to the Washington Double Star Catalog, according to several criteria:

- The Right Ascension (RA) of the star was constrained to be within the optimal RA of 3 to 13 hours at the time of measurement in January.
- The secondary star was constrained to have a magnitude less than 13 in order to be detectable with the equipment used.
- The difference in the magnitude of the two stars (Δmag) was constrained to be less than 3 so that both stars could be captured in the same image.
- The constraint for the lower bound of the two star's separation was 5 arcseconds so that the two stars could be resolved, and the constraint for the upper bound was 15 arcseconds as it is more likely for two stars close together to be related in some way.
- Systems marked as "physical" according to Stelle Doppie were selected because these are more likely to have a similar parallax and proper motion.

Table 1 provides the Discoverer code, WDS number, and astrometric measurements for the three systems, along with colors and apparent Gaia G-filter magnitudes from Gaia Data Release 3 (DR3), and estimated spectral types and masses. The latter are estimated by plotting the stars' colors and absolute Gaia G-magnitudes (computed from apparent G-magnitude and parallax according to Equation 1) on the Gaia HR-

Diagram in Fig. 1 (Gaia Collaboration, 2023, 2016b, 2023j). Note that the parallax values cited in Fig. 1 are listed with their uncertainties in Table 5.

Table 1. Double Star System Summary Data.

System	WDS	Star (Primary / Secondary)	Spectral Type	Estimated Mass (solar masses)	Last Observation Date	Last observed PA (deg)	Last observed Sep (arcsecs)
HJ 4258	09448 -7554	Primary	F7[1]	1.2	2016[2]	163	8.62
		Secondary	F[1]	1.1			
STF 1106	07313 +1619	Primary	F0	1.4	2017.222[3]	33.9	10.68
		Secondary	F0	1.3			
VNI 1	04534 +0452	Primary	K	0.66	2015.5	51.67	9.65
		Secondary	M	0.46			

[1] Houk et al. (1975)
[2] El-Badry et al. (2021)
[3] Mason et al. (2018)

The mass of the two stars of each system was estimated by plotting the absolute magnitude and color on a CMD diagram. The absolute magnitude was calculated using Eq. 1 and the parallax, magnitudes (gmag), and color (BP-2P) were taken from Gaia DR3 (Collaboration, 2023, 2016b, 2023j).

Table 2. Gaia DR3 data of double star systems.

System		Plx (mas)	gmag	BP-RP
HJ 4258	pri	4.57	8.95	0.93
	sec	4.57	9.67	0.84
STF 1106	pri	6.66	9.26	0.74
	sec	6.55	9.32	0.71
VNI 1	pri	16.97	10.28	1.23
	sec	17.07	12.02	1.89

$$M = m + 5 \cdot log(p + 1)$$

Equation 1: Gaia G absolute magnitude (M) from gmag (m) and parallax (p)

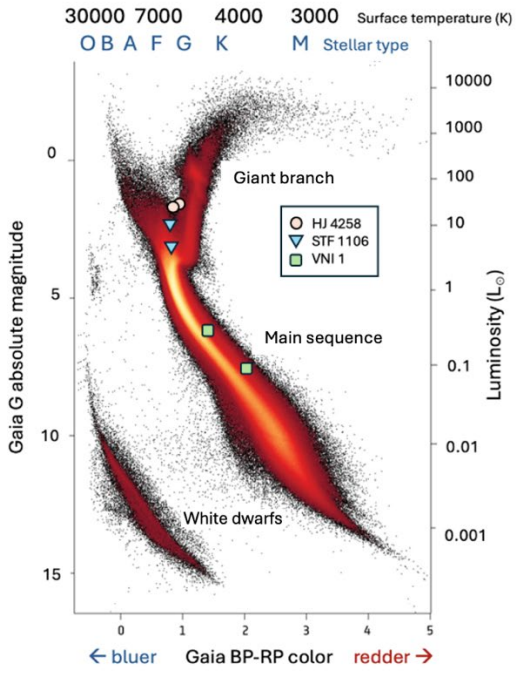

Figure 1: Information from Gaia DR3 of the double star systems HJ4258, STF1106, and VNI1

The stars of HJ 4258 are high proper motion stars (Wenger et al., 2000) of approximately solar mass. When plotted on Gaia's CMD diagram, the stars of HJ 4258 are found to be close to the main sequence turnoff point. The stars of VNI 1 are still definitively on the main sequence, while STF 1106's position relative to the giant branch is inconclusive.

Notably, STF 1106 is the only system of this study considered to have wide (> 1 pc) separation, at 2.54 pc. This is the 3D spatial separation as shown in Table 6, calculated through the process described in Sec. 4. Past studies have shown that it is difficult to distinguish whether comoving double stars with > 1 pc separation are genuine binaries, separated former binaries, moving groups, or contamination from randomly aligned stars (Andrews et al., 2017).

Finally, VNI 1 is the only system studied with significantly different masses— the secondary star mass is 30% less than that of the primary star whereas the mass difference for the pairs of stars of STF 1106 and HJ 4258 are both less than 10%, using the estimated masses from Table 1. The two stars of VNI 1 also have the highest parallax within the study of 16.97 and 17.07, meaning the two stars are within 60 parsecs of Earth.

None of the systems studied have a published orbital or linear solution. Therefore, in addition to contributing to astrometric data and using the computed system escape velocities to classify each system, we aim to examine the historical data to ascertain whether either of these solution types are relevant.

2. Equipment and Methods

Images were requested from telescopes in the Las Cumbres Observatory Global Telescope (LCOGT) network (Brown, 2013). All telescopes were DeltaRho 350 telescopes with aperture 0.35m using a QHY600PH CMOS camera. The camera's field of view is 1.9 x 1.2 degrees, but this is cut down to 30′ x 30′ in the central mode used for imaging to minimize file size. Pixel size is 3.76 microns covering 0.73″ per pixel. Images were taken using a V filter (Bessell, 1990). Observing site, decimal date, and exposure time are listed in Table 3.

Table 3. Telescope Observing Parameters.

System	Telescope Location	Observation Date	Exposure Time per image (s)
HJ 4258	Sutherland, South Africa	2024.0301	3.80
STF 1106	Texas, USA	2024.0356	4.00
VNI 1	Siding Spring, Australia	2024.0342	7.78

10 telescope images of each system were reduced to determine astrometric position angle (PA, in degrees) and separation (Sep, in arcseconds) by centroiding in AstroImageJ. Plotting these measurements along with historical data reveals trends in relative motion (Fig. 2).

Fig. 2 below depicts an example of a resolved image of each system using AstroImageJ.

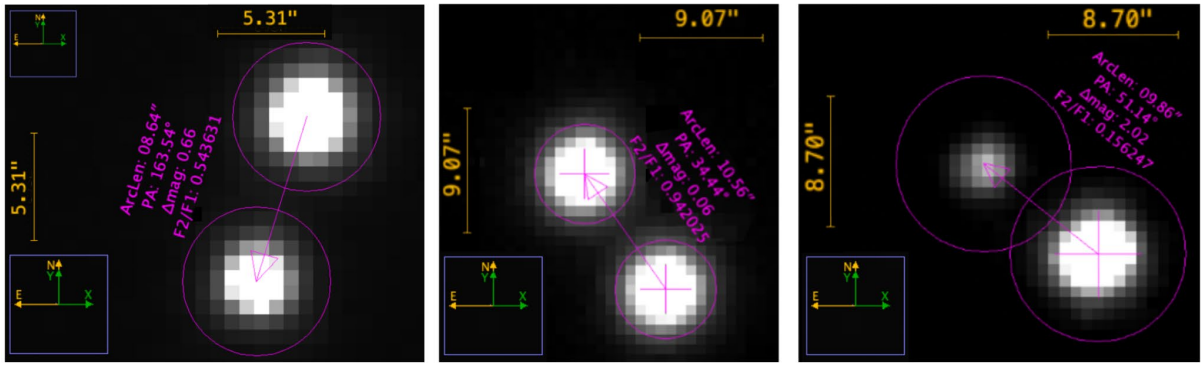

Figure 2: Example measurements in AstroImageJ of PA and Sep for systems from left to right: HJ 4258 (measurement aperture radius 5 pixels), STF 1106 (5 pixels), and VNI 1 (8 pixels)

3. Data

Table 3 below shows measurements of 10 images for each of the double star systems HJ 4258, STF 1106, and VNI 1. All image reductions were performed using AstroImageJ.

Table 3. Astrometric Measurement of Position Angle and Separation of Star Systems.

	HJ 4258		STF 1106		VNI 1	
Image #	PA (deg)	Sep (arcsecs)	PA (deg)	Sep (arcsecs)	PA (deg)	Sep (arcsecs)
1	163.0	8.65	34.1	10.68	51.0	9.53
2	163.5	8.56	33.9	10.68	50.2	9.58
3	162.9	8.62	34.1	10.69	51.1	9.71
4	163.0	8.61	34.0	10.69	51.2	9.11
5	163.5	8.61	34.1	10.67	51.3	9.72
6	163.2	8.59	34.5	10.60	50.9	9.59
7	163.4	8.92	34.4	10.56	50.2	9.66
8	163.1	8.63	33.9	10.72	50.5	9.79
9	163.2	8.62	34.1	10.68	53.1	9.74
10	163.2	8.65	34.2	10.64	53.7	9.66

Table 4 shows summary statistics for the measurements above, including the mean, standard deviation (SD), and standard error (SE) for the position angle and separation of the three double star systems.

Table 4. Summary of Measurements of HJ 4258, STF 1106, and VNI 1.

System	Date of Measurement	Number of Images	Position Angle (°)	Standard Deviation of Position Angle	Standard Error of Position Angle	Separation (")	Standard Deviation of Separation	Standard Error of Separation
HJ 4258	2024.0301	10	163.2	0.19	0.060	8.65	0.10	0.032
STF 1106	2024.0356	10	34.1	0.20	0.063	10.66	0.05	0.015
VNI 1	2024.0342	10	51.3	1.18	0.373	9.61	0.19	0.061

4. Escape Velocity versus Relative Velocity

The masses shown in Table 1 were used to calculate an escape velocity for each double star system. The formula for escape velocity (Eq. 2) is derived by finding the relative velocity of orbit such that the total mechanical energy of the system is 0 (Bonifacio et al., 2020). In Eq. 2, *M* is the sum of the masses of the two stars, with units converted from solar masses to kg. *r* is the 3D spatial separation between the two stars, with units converted from parsecs to meters. Hence the escape velocity is in meters per second.

$$\mathrm{v}_{escape} = \sqrt{\frac{2GM}{r}}$$

Equation 2: Escape velocity

The 3D spatial separation (r) in Eq. 2 was calculated from the stars' angular astrometric Sep (Table 4) and radial separation computed by taking the difference of the inverted Gaia DR3 parallaxes in arcseconds (Table 5). The angular separation (in arcseconds) was converted into physical separation (Sep_{pc} in parsecs) through the following formula, where parallax is abbreviated as Plx, and separation is abbreviated as Sep_{arcsec}.

$$\mathrm{Sep}_{pc} = \frac{\mathrm{Sep}_{arcsec} \cdot \frac{1(\mathrm{deg})}{3600(\prime\prime)} \cdot \frac{2\pi(\mathrm{rad})}{360(\mathrm{deg})}}{\mathrm{Plx}(\prime\prime)}$$

Equation 3: Transverse separation in parsecs

For each system, the parallax used to compute the transverse separation in Eq. 3 was the Gaia DR3 primary star parallax shown in Table 5. The 3D separation was computed as the transverse and radial separation combined via the Pythagorean Theorem. Since the parallax uncertainties for HJ 4258 were overlapping, the 3D separation was taken as the transverse separation without any radial component. Table 5 shows the parallax, proper motion in right ascension (RA) and declination (Dec), and radial velocity for each star (Gaia Collaboration, 2023, 2016b, 2023j).

Table 5. Gaia DR3 Parallaxes, Proper Motions, and Radial Velocities.

System	Star	Parallax (mas)	Proper Motion RA (mas/yr)	Proper Motion Dec (mas/yr	Radial Velocity (km/s)
HJ 4258	Primary	4.57 ± 0.011	-56.77 ± 0.015	27.92 ± 0.014	N/A
	Secondary	4.57 ± 0.023	-57.45 ± 0.030	28.37 ± 0.027	-1.14 ± 0.0266
STF 1106	Primary	6.66 ± 0.020	16.92 ± 0.024	-21.16 ± 0.019	-10.51 ± 6.271
	Secondary	6.55 ± 0.015	17.89 ± 0.019	-21.49 ± 0.015	-2.74 ± 0.300
VNI 1	Primary	16.97 ± 0.019	-43.83 ± 0.024	-65.82 ± 0.017	14.08 ± 0.206
	Secondary	17.07 ± 0.017	-45.59 ± 0.019	-65.63 ± 0.015	15.26 ± 0.376

The proper motions in Table 5 were also used to compute the relative 3D space velocity of the system for comparison with the escape velocity. The 3D space velocity is calculated with the Pythagorean theorem from the radial velocity (where available) and proper motion changes from angular to physical units via Equation 3. As shown in Table 6, HJ 4258 has a slower relative velocity than escape velocity according to this analysis and therefore is likely to be gravitationally bound. Although unlikely to be bound, STF 1106 and VNI 1 are physically related, as evidenced by their low relative proper motion ratio (rPM). The rPM is calculated as the ratio of the relative proper motion to the longer proper motion vector magnitude of the two stars. A small ratio indicates that the motion of the secondary star with respect to the primary is small compared to the movement of the system as a whole, so the two stars are mostly moving together. A double star system is classified as Common Proper Motion (CPM) if its relative proper motion ratio is between 0 and 0.2, as is the case for all of these systems (Harshaw, 2016).

Table 6. System Separation and Classification based on Relative Proper Motion Ratio.

System	3D Spatial Separation (pc)	System Escape Velocity (m/s)	3D Relative Velocity (m/s)	Relative Proper Motion (rPM) ratio	Classification based on rPM
HJ 4258	0.01	1473	842	0.013	CPM
STF 1106	2.54	96	7805	0.04	CPM
VNI 1	0.31	175	1279	0.022	CPM

Figure 3 below shows the historical data plots of the relative position in right ascension and declination of the secondary star with respect to the primary for star systems HJ 4258, STF 1106, and VNI 1. In these plots, the primary star is located at the origin of the RA/Dec coordinate system. The blue square represents the data point calculated from this study using the 10 images, and the red circle represents Gaia DR3 data (epoch 2016.0). Time is shown on a gradient from purple to yellow, with most recent measurements yellow and the earliest purple. Two outliers were removed from the plot of STF 1106 because they had a PA of

75 where all other data points had a PA in the value range from 25 to 35, and a separation of 8.24 where all other measurements were in the range from 10 to 11.5.

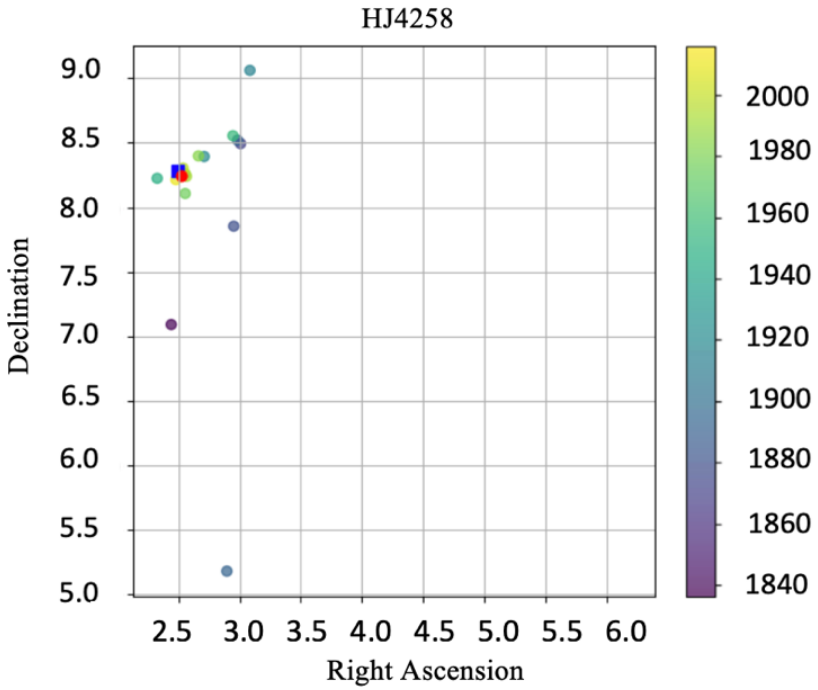

Figure 3a: Relative position of secondary star with respect to the primary of HJ 4258

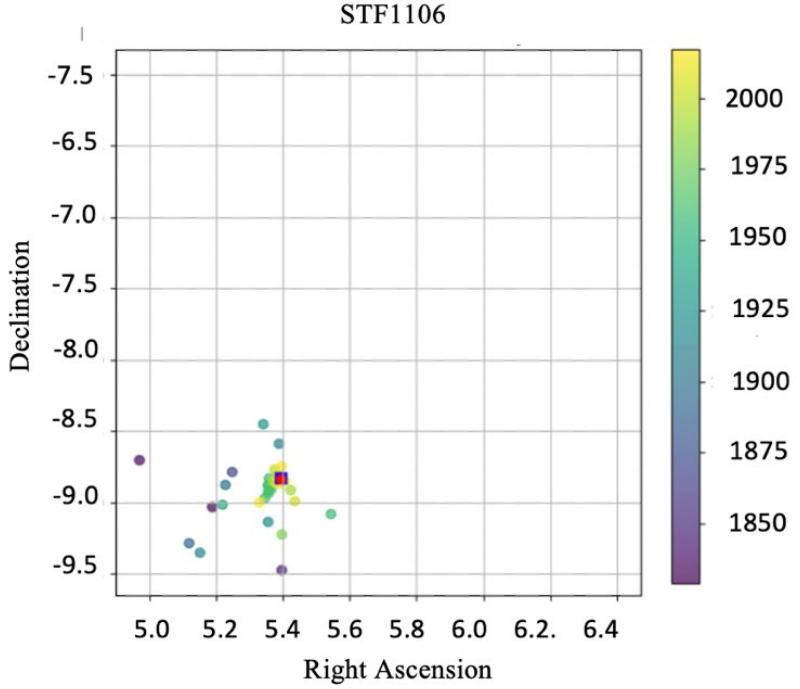

Figure 3b: Relative position of the secondary star in with respect to the primary of STF 1106

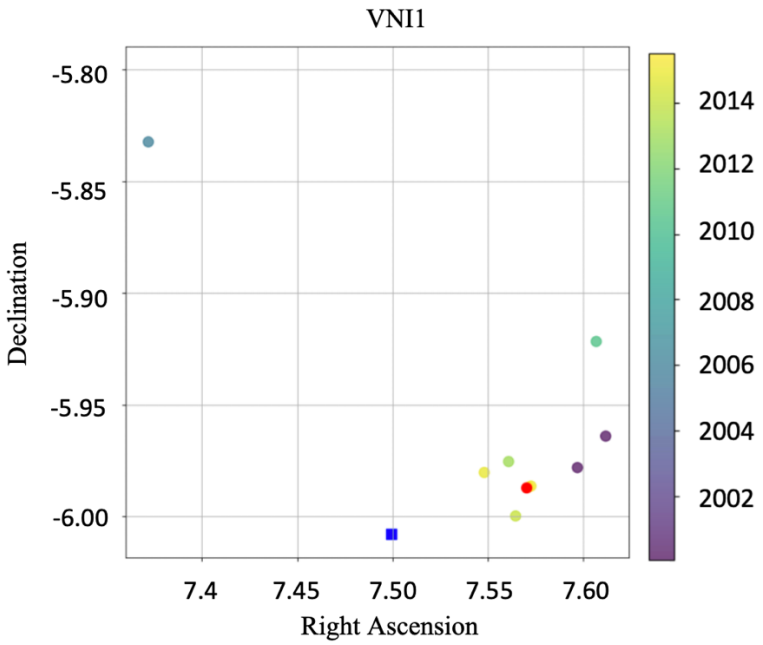

Figure 3c: Relative position of the secondary star with respect to the primary star of VNI 1

5. Discussion

In the plot of HJ 4258 (Fig. 3a), although many of the older measurements are sparse and show high imprecision, varying from each other in an unlikely manner, the measurements could be interpreted to suggest a possible elliptical orbit going from the bottom of the graph upwards to the upper right, and turning back left and down. However, when scaling the axes to include the origin, this possible elliptical orbit does not appear to contain the origin, so it would not be a reasonable orbital path as the origin represents the primary star's location. Assuming that the oldest measurements were inaccurate, there would be a trend of decreasing Dec and gradually decreasing RA in the more recent measurements, which may indeed represent an orbit around the primary star. The newest measurement of this study does continue the recent trend of moving generally leftward in the plots. There may be some slight curvature downward to the origin, but this would require future measurements to confirm.

Most of the recent measurements of STF 1106 (colored green and yellow in the second plot of Fig. 3b) are clumped together while older measurements exhibit no trend. Similar to the data points of HJ 4258, this may be due to lack of precision of older measurements. However, over time, the secondary star tends to move in the positive direction in both Dec and RA. As shown in Fig. 3b, older data points tended to be to the left and bottom (more negative Dec and smaller RA) while the more recent data tended to be more upwards and to the right, and this study's measurement is at the center of a clump of recent measurements.

For VNI 1, notably are three overlapping data points at where the red circle is marked. The three measurements were all taken in 2015. When 11 data points were plotted, there is a general trend of the relative position of the secondary star decreasing in Right Ascension and Declination, implying that the secondary star is moving nearer to the primary star.

The historical data of all three systems indicate trends in the relative position of the secondary star, but no conclusive orbital path. There is also currently no published orbital solution for any of the three double star systems, suggesting more measurements are needed to determine how the secondary star's relative position changes over time. Using the measurements from Table 6, only HJ 4258 has a relative 3D space velocity which does not exceed its escape velocity. The other two systems, STF 1106 and VNI 1, each have a relative velocity which exceeds the system escape velocity by 2 orders of magnitude, so they are unlikely to be gravitationally bound. This makes HJ 4258 the only system in this study where an orbital relationship is likely.

However, while only HJ 4258 is likely to have an orbital relationship, all three double star systems exhibit common proper motion. STF 1106, with its physical separation of 2.54pc (Table 6), is considered a comoving pair of stars with a wide separation (> 1 pc) by Oh et al., 2017. Therefore, it may be a separated former binary, and could be potentially used to measure the star formation and evolution in the solar neighborhood (Oh et al., 2017).

6. Conclusion

Astrometric data analysis shows that all three systems studied here exhibit common proper motion, suggesting a physical relationship between the primary and secondary star of each system. Escape velocity calculations and comparisons with 3D space velocity indicate that only HJ 4258 is likely to be gravitationally bound, though there is no evidence of this in its historical data plot. The components of VNI 1 and STF 1106 are likely to be physically related (despite STF 1106's wide separation of 2.54pc) but not gravitationally bound. The measurements presented in this paper plot close to Gaia DR3 measurements, and continue temporal trends identified for VNI 1 and STF 1106. Further observations over time are recommended for all three systems.

Acknowledgements

This research was made possible by the Washington Double Star catalog maintained by the U.S. Naval Observatory, the Stelledoppie catalog maintained by Gianluca Sordiglioni, Astrometry.net, and AstroImageJ software which was written by Karen Collins and John Kielkopf.

This work has also made use of data from the European Space Agency (ESA) mission Gaia (https://www.cosmos.esa.int/gaia), processed by the Gaia Data Processing and Analysis Consortium (DPAC, https://www.cosmos.esa.int/web/gaia/dpac/consortium). Funding for the DPAC has been provided by national institutions, in particular the institutions participating in the Gaia Multilateral Agreement.

This work makes use of observations taken by the Planewave Delta Rho 350 + QHY600 CMOS camera systems of Las Cumbres Observatory Global Telescope Network located in Coonabarabran, Australia; Texas, USA; and Sutherland, South Africa.

References

Andrews, J. J., Chanamé J., Agüeros, M. A. (2017). Wide binaries in Tycho-*Gaia*: search method and the

distribution of orbital separations, *Monthly Notices of the Royal Astronomical Society*, Volume 472, Issue 1, Pages 675–699, https://doi.org/10.1093/mnras/stx2000

Banik, I., Pittordis, C., Sutherland, W., Famaey, B., Ibata, R., Mieske, S., & Zhao, H. (2024). Strong constraints on the gravitational law from Gaia DR3 wide binaries, Monthly Notices of the Royal Astronomical Society, Volume 527, Issue 3, Pages 4573–4615, https://doi.org/10.1093/mnras/stad3393

Bessell, M.S. (1990). UBVRI Passbands. Publications of the Astronomical Society of the Pacific, 102, 1181-1199. https://iopscience.iop.org/article/10.1086/132749

Bonifacio, B., Marchetti, C., Caputo, R., & Tock, K. (2020). Measurements of Neglected Double Stars. Journal of Double Star Observations, 16(5), 411–423. http://www.jdso.org/volume16/number5/Bonifacio_411_423.pdf

Brown, T. M., et al. (2013). Las Cumbres Observatory Global Telescope Network. Publications of the Astronomical Society of the Pacific, 125(931), 1031–1055. https://iopscience.iop.org/article/10.1086/673168/meta

El-Badry, K., Rix, H., & Heintz., T. M. (2021). A million binaries from Gaia eDR3: sample selection and validation of Gaia parallax uncertainties. Monthly Notices of the Royal Astronomical Society, 506(2), 2269-2295. 10.1093/mnras/stab323

Gaia Collaboration, Babusiaux, C., Fabricius, C., Khanna, S., et al. (2023). Gaia Data Release 3. Catalogue validation. A&A 674, pp. A32. https://arxiv.org/abs/2206.05989

Gaia Collaboration, Prusti, T., de Bruijne, J.H.J., et al. (2016b). The Gaia mission. A&A 595, A1. https://www.aanda.org/articles/aa/full_html/2016/11/aa29272-16/aa29272-16.html

Gaia Collaboration, Vallenari, A., Brown, A.G.A., et al. (2023j). Gaia Data Release 3. Summary of the content and survey properties. A&A 674, pp. A1. https://arxiv.org/abs/2208.00211

Harshaw, R. (2016). CCD Measurements of 141 Proper Motion Stars: The Autumn 2015 Observing Program at the Brilliant Sky Observatory, Part 3. Journal of Double Star Observations, 12(4), 394–399. http://www.jdso.org/volume12/number4/Harshaw_394_399.pdf

Houk, N., Cowley, A.P. (1975). University of Michigan Catalogue of two-dimensional spectral types for the HD stars. Volume 1. Declinations -90 to -53_*f*0. Ann Arbor, MI (USA): Department of Astronomy, University of Michigan, 19 + 452 p.

Mason et al., (2018). Speckle Interferometry at the U.S. Naval Observatory. XXIII, The Astronomical Journal, 156 (5), 240. 10pp. https://iopscience.iop.org/article/10.3847/1538-3881/aae484/pdf

Oh, S., Price-Whelan, A. M., Hogg, D. W., Morton, T. D., & Spergel, D. N. (2017). Comoving Stars in Gaia DR1: An Abundance of Very Wide Separation Comoving Pairs. The Astronomical Journal, 153(6), 257. https://doi.org/10.3847/1538-3881/aa6ffd

Wenger, M., et al. (2000). The SIMBAD Astronomical Database. Astronomy and Astrophysics Supplement Series, 143(1). https://doi.org/10.1051/aas:2000332